

Supporting Information

Ferrarelli et al. 10.1073/pnas.0913008107

SI Methods

TMS Neuronavigation. TMS was performed by means of a 70-mm figure-of-eight coil, connected to a Magstim Rapid biphasic stimulator. The targeted cortical area, the right premotor cortex, was identified on each subject's T1 anatomical MRI, acquired with a 3-T GE scanner. The TMS coil was placed on the corresponding scalp position, about 1 cm anterior and lateral of the Cz electrode. To ensure precision and reproducibility of stimulation, we used a portable Brain Navigated Stimulation system (Softaxic; E.M.S.). The Softaxic neuronavigational system located (with an error of ≤ 3 mm) the relative positions of the subject's head and of the TMS coil by means of an optical tracking system (Polaris Vicra; NDI). It also calculated the distribution and strength of the TMS-evoked intracranial electric field, including the area on the cortical surface where the electric field was maximal (hot spot). During the TMS procedure, the coordinates of stimulation were constantly monitored, to ensure the reproducibility of position, direction, and angle of the stimulating coil. The intensity of the stimulator output was based on the maximum TMS-induced electric field on the cortical surface, calculated by the navigated brain stimulation system and expressed in volts per meter (V/m). By calibrating TMS intensity based on the estimated electric cortical field, rather than relying on the percentage of maximum stimulator output, we ensured that in each subject the premotor cortex was stimulated at comparable intensities, despite interindividual differences in scalp-to-cortex distance and anatomy. This assumption was confirmed when identifying, in each subject, the resting motor threshold (RMT), defined as the TMS intensity required to evoke a ≥ 50 - μ V electromyographic response in 5 of 10 consecutive trials, in the relaxed, left first-dorsal interosseus muscle. Indeed, we found that individual RMT, a measure of cortical excitability, ranged from 55% to 69% of TMS stimulator output (mean = 62.5%, SD = 5.5%). These RMT values were highly correlated with the individual scalp-to-cortex distance ($r = 0.98$, $P = 0.0002$) and, when accounting for the distance between the coil and the motor cortical surface, we found that TMS-evoked electric fields were very similar across subjects (mean EF = 102 V/m, SD = 4). Based on the finding that EF ~ 100 V/m corresponded to the RMT, as reported by another recent study (1), an intensity of 120 V/m was chosen to compare the TMS-evoked brain responses during wakefulness and anesthesia.

High-Density (hd)-EEG Recording During TMS. TMS-evoked EEG responses were recorded by using a TMS-compatible 60-channel amplifier (Nexstim), provided with a proprietary sample-and-hold circuit to gate TMS pulses and prevent saturation (2). The EEG signals, referenced to an additional electrode on the forehead, were filtered (between 0.1 and 500 Hz) and sampled at 1,450 Hz with 16-bit resolution. Two extra sensors were used to record the electrooculogram. In most cases, no TMS-induced magnetic artifact was detected, and in all recordings, EEG signals were artifact-free from 8 ms after the TMS stimulus (3). To further improve TMS compatibility, the impedance at all electrodes was kept below 3 K Ω . To prevent contamination of the TMS-evoked EEG potentials with the auditory response to the TMS click sound, subjects wore earphones through which a masking noise, reproducing the time-varying frequency components of the TMS click, was played. Before starting the experiment, we delivered single TMS pulses, and the volume was adjusted until the subject reported that the TMS click was not audible. Noise masking was then played during the TMS sessions. Bone conduction was attenuated by placing a thin layer of foam between the TMS coil and the scalp. These procedures have been successfully employed to abolish the auditory potentials evoked by the TMS click sound in previous studies from our group (4–6).

Data Analysis and Statistics. Data analysis was performed with MATLAB (MathWorks). TMS trials containing artifacts, including muscle activity or eye movements, were automatically detected and rejected. EEG data were then average referenced, down-sampled from 1,450 Hz to 725 Hz, and band-pass-filtered (2–80 Hz). Source modeling analysis, aimed at identifying the cortical currents underlying the TMS-evoked EEG scalp potentials, was performed as follows. The free-license software SPM (www.fil.ion.ucl.ac.uk/spm) was used to create a model of the cerebral cortex as a three-dimensional grid of 3,004 fixed dipoles oriented normally to the cortical surface. This model, based on the average Montreal Neurological Institute (MNI) cortex, was adapted to the anatomy of each subject in three steps. First, binary masks of the skull and scalp obtained from individual MRIs were warped to the corresponding standard MNI cortical meshes. Then, an inverse transformation (from standard to individual data) was applied to the MNI cortical meshes for approximating individual real anatomy. Finally, EEG scalp sensors and individual cortical meshes were coregistered by rigid rotations and translations of digitized landmarks (nasion, left, and right tragus). The inverse solution, which estimates the cortical current sources underlying EEG scalp potentials, was calculated on a single trial basis by applying an “empirical” Bayesian approach (7–9). Current sources were calculated at individual cortical meshes (vertices), and the corresponding cortical regions (Brodmann areas) were identified by using an automatic tool of anatomical classification (WFU PickAtlas tool). After source modeling analysis, a statistical procedure to assess where and when the TMS-evoked cortical response was significantly different from prestimulus EEG activity was employed. Specifically, because of the large number (3,004) of cortical sources, which increased the occurrence of false positives, a nonparametric permutation-based procedure was selected (10). This procedure assumes that, under the null hypothesis of no effect of TMS, mean cortical activity in the original dataset will not be different from the mean activity resulting from a random permutation of pre- and post-stimulus periods. Thus, for each permuted “new” dataset, the corresponding average cortical response was computed and compared with the average of the original dataset. Before comparison, average responses at each cortical source were normalized by subtracting the mean prestimulus value and dividing by prestimulus variance, to allow for equal weighting of sources in the statistical analysis. Significance threshold for the multiple comparison procedure was set at $\alpha = 0.01$, estimated over 1,000 permutations. This method allowed identification of the spatial and temporal distribution of TMS-evoked statistically significant cortical currents. From these cortical currents, two synthetic indexes of brain responsiveness to TMS, significant current density (SCD) and significant current scattering (SCS), were computed (11). SCD, which captures the strength of the TMS-evoked cortical currents, was calculated by cumulating the absolute amplitude of all of the significant cortical currents evoked by TMS over a time interval σ (i.e., 0–500 ms post-TMS) and for each (significantly activated) cortical region s . SCS, which represents the spatial scattering of the TMS-evoked significant activations, was computed by cumulating the geodesic distance between any significant current source and the TMS cortical target over a time range σ (first 500 ms post-TMS) and each (significantly activated) cortical region s . Although SCD_{σ} is a single value reflecting the total current evoked by the TMS and is therefore maximally sensitive to the magnitude of the evoked cortical activations, SCS_{σ} is largely determined by the spatial spreading of the TMS-evoked responses, thus reflecting cortical activity occurring far away from the stimulation site.

1. Thielscher A, Kammer T (2002) Linking physics with physiology in TMS: a sphere field model to determine the cortical stimulation site in TMS. *Neuroimage* 17:1117–1130.
2. Ilmoniemi RJ, et al. (1997) Neuronal responses to magnetic stimulation reveal cortical reactivity and connectivity. *Neuroreport* 8:3537–3540.
3. Virtanen J, Ruohonen J, Näätänen R, Ilmoniemi RJ (1999) Instrumentation for the measurement of electric brain responses to transcranial magnetic stimulation. *Med Biol Eng Comput* 37:322–326.
4. Ferrarelli F, et al. (2008) Reduced evoked gamma oscillations in the frontal cortex in schizophrenia patients: a TMS/EEG study. *Am J Psychiatry* 165:996–1005.
5. Massimini M, et al. (2007) Triggering sleep slow waves by transcranial magnetic stimulation. *Proc Natl Acad Sci USA* 104:8496–8501.
6. Massimini M, et al. (2005) Breakdown of cortical effective connectivity during sleep. *Science* 309:2228–2232.
7. Friston KJ, et al. (2002) Classical and Bayesian inference in neuroimaging: theory. *Neuroimage* 16:465–483.
8. Mattout J, Phillips C, Penny WD, Rugg MD, Friston KJ (2006) MEG source localization under multiple constraints: an extended Bayesian framework. *Neuroimage* 30: 753–767.
9. Phillips C, Mattout J, Rugg MD, Maquet P, Friston KJ (2005) An empirical Bayesian solution to the source reconstruction problem in EEG. *Neuroimage* 24:997–1011.
10. Pantazis D, Nichols TE, Baillet S, Leahy RM (2003) Spatiotemporal localization of significant activation in MEG using permutation tests. *Inf Process Med Imaging* 18: 512–523.
11. Casali AG, Casarotto S, Rosanova M, Mariotti M, Massimini M (2010) General indices to characterize the electrical response of the cerebral cortex to TMS. *Neuroimage* 49: 1459–1468.

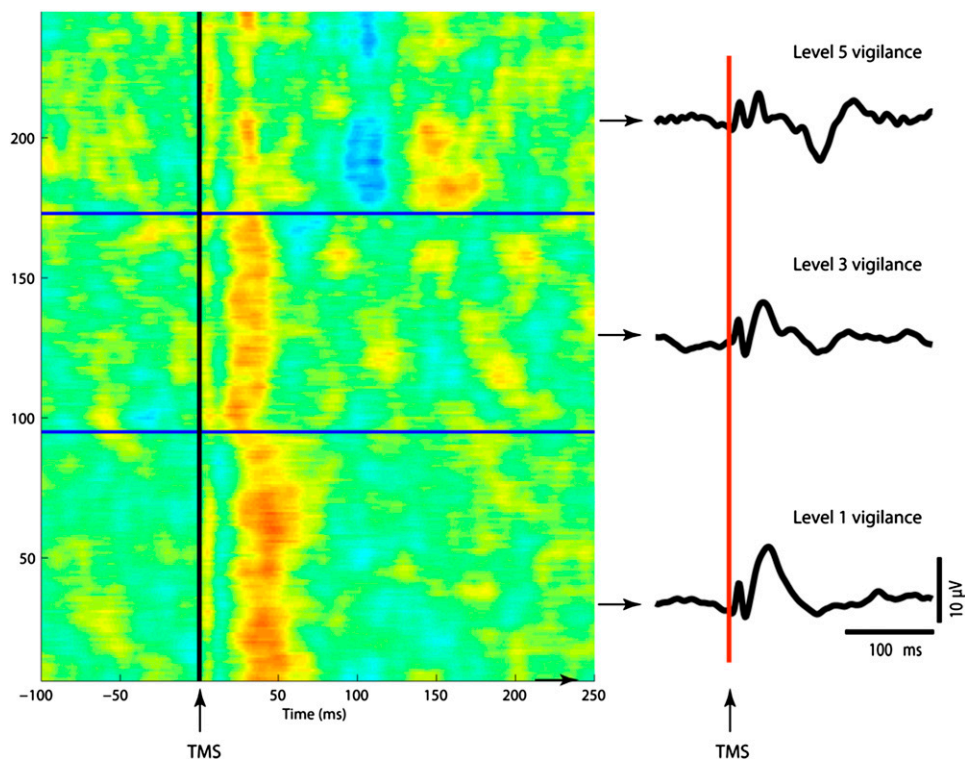


Fig. S1. Changes in TMS-evoked brain responses while transitioning from high ($OAA/S = 5$) to low ($OAA/S = 1$) levels of vigilance. (Left) Single trials recorded from one channel located under the TMS coil. Single-trial EEG data (filtered from 4 to 100 Hz) are color-coded for voltage. (Right) Averaged TMS-evoked responses (filtered from 1 to 100 Hz) obtained during the three levels of vigilance. Both single and average EEG responses showed a progressive increase in the amplitude and latency of an early evoked component (positive peak), followed by the obliteration of succeeding oscillations when reaching low levels of vigilance.

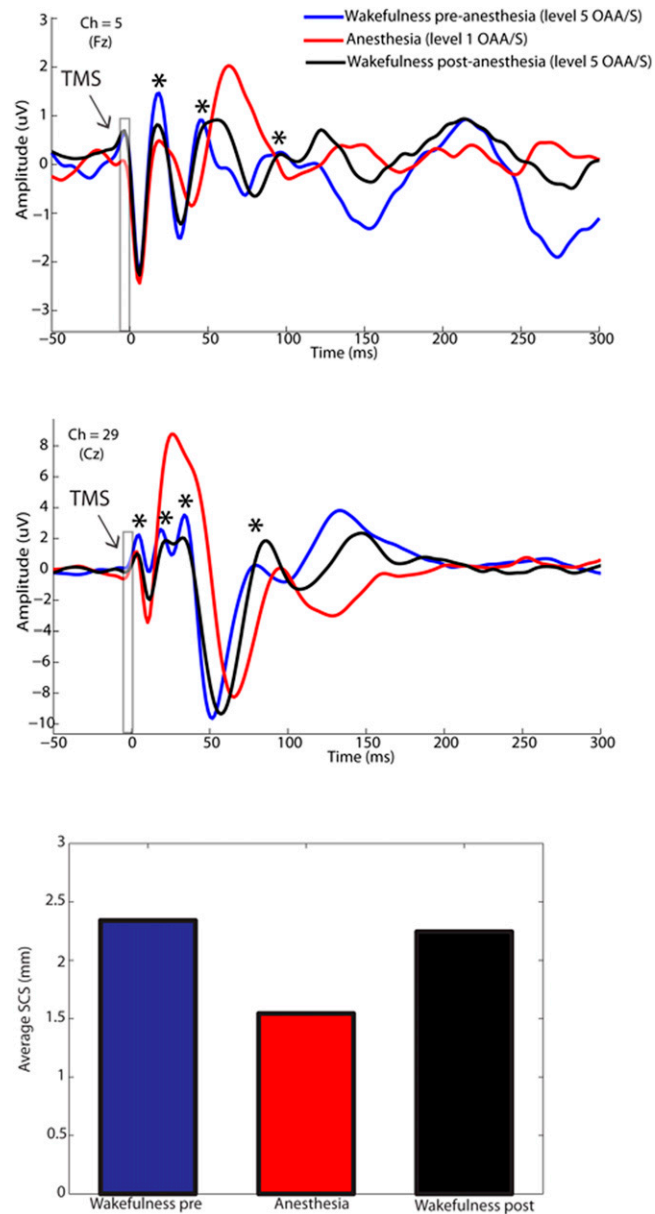


Fig. S2. Recovery from midazolam-induced LOC. (*Upper*) TMS-evoked EEG responses in the recovery from midazolam were largely overlapping with the EEG potentials recorded before midazolam injection, whereas they were clearly different from the TMS-evoked responses during midazolam-induced LOC. Average EEG responses from Cz, an electrode close to the stimulated cortical area (premotor cortex, BA 6), and Fz, an electrode overlying a cortical area (BA 8) anatomically connected with BA 6. Asterisks indicate the fast oscillations occurring in the first 50–100 ms during the wakefulness pre-LOC (blue traces) and post-LOC (black traces) conditions, but not during LOC (red traces). (*Lower*) Mean SCS, a measure of cortical connectivity, was similar between the wakefulness (SCS = 2.35) and recovery (SCS = 2.3), whereas it dropped during LOC (SCS = 1.5).